Peptidyl Aldehydes as Reversible Covalent Inhibitors of Src Homology 2 Domains†

Junguk Park, Hua Fu, and Dehua Pei*

Department of Chemistry and Ohio State Biochemistry Program, The Ohio State University, 100 West 18th Avenue, Columbus, Ohio 43210

Received January 15, 2003

ABSTRACT: Src homology 2 (SH2) domains are phosphotyrosine- (pY-) binding modules found in a variety of signal-transducing proteins and constitute an important class of drug targets for the treatment of signaling related diseases/conditions. To date, a large number of peptidic as well as nonpeptidic SH2 domain inhibitors have been reported. However, all of these inhibitors contain a negatively charged pY mimetic as the core structure and generally have poor membrane permeability. We report here that peptidyl cinnamaldehydes function as reversible, slow-binding inhibitors toward the SH2 domains of protein tyrosine phosphatase SHP-1. Specific interactions between the SH2 domains and the aldehydes were assessed by their ability to relieve the autoinhibitory effect of the N-terminal SH2 domain on SHP-1 catalytic activity and the surface plasmon resonance technique. The most potent inhibitor (Cinn-GEE) displayed a K_D value of 1.3 μM against the N-terminal SH2 domain of SHP-1. The mechanism of inhibition was investigated by site-directed mutagenesis and by using Cinn-GEE specifically labeled with ^{13}C at the aldehyde carbon and $^{1}H-^{13}C$ heteronuclear single-quantum coherence spectroscopy. The proposed mechanism involves the formation of an initial noncovalent E·I complex, which is slowly converted into a covalent imine/enamine adduct (E·I*) between the aldehyde group of the inhibitor and the guanidine group of Arg βB5 in the pY-binding pocket of the SH2 domains. These aldehydes should provide a general, neutral pharmacophore for the further development of potent, specific, and membrane-permeable SH2 domain inhibitors.

Protein−protein interaction is an important aspect of cellular processes. Many of these interactions are mediated by small modular domains, which recognize peptide motifs in their partner proteins. The Src homology 2 (SH2) domain was one of the first such modular domains identified (*1*). Since then, dozens of other modules have now been discovered (e.g., SH3, PH, PDZ, FHA, and PTB domains) (*2*). SH2 domains contain ∼100 amino acids and are often found in signaling proteins. A large number of SH2 domains have already been identified, and the human genome encodes at least 95 SH2 domains (*3*). Their function is to bind specific phosphotyrosine- (pY-)[1] containing proteins and promote protein−protein interactions. The structural basis for SH2 domain−pY interaction has been very well studied. SH2 domains bind to their partner proteins by recognition of linear pY-containing sequence motifs (*4*, *5*). A key interaction, which is common to all SH2 domains, is the insertion of the pY side chain into a deep pocket in the SH2 domain, where an invariant arginine residue (Arg βB5) forms a bidentate interaction with the pY phosphate group (*6*−*9*). Additional binding energy is provided by interactions between amino acids adjacent to pY, particularly the three residues immediately C-terminal to pY, and the less conserved surface of the SH2 domain. This latter interaction also governs the selectivity of a given SH2 domain in binding to a specific pY partner.

The blockade of SH2 domain-dependent protein−protein interactions has emerged as a new strategy for treating a plethora of diseases related to cell signaling, such as cancer, osteoporosis, allergy, asthma, and inflammation (*10*). A variety of inhibitors have been developed against the SH2 domains of Src kinase and adapter protein Grb2 (reviewed in refs *10* and *11*). A Src SH2 domain inhibitor (AP22408) has been shown to reduce the bone resorptive activity of osteoclasts in rat (*12*). In addition to their therapeutic values, SH2 domain inhibitors also provide useful probes for elucidating the cellular function of the SH2 domain-containing protein.

Since the natural ligands of SH2 domains are pY peptides, there are two challenges in designing SH2 domain inhibitors. The first is to find a proper small-molecule replacement for the peptide backbone, whereas the second is to design pY isosteres that are capable of interacting with the highly positively charged pY-binding pocket and yet have the desired pharmacological properties (e.g., membrane permeability). The first challenge has largely been overcome, as evidenced by the availability of many potent, nonpeptidic SH2 inhibitors (*11*). On the other hand, finding the proper pY isostere has been much more difficult. All of the reported

† This work was supported by grants from the National Institutes of Health (AI40575 and GM62820). The BIAcore instrument was supported by an NIH grant (RR15895; Dr. Charles Brooks, Principal Investigator).

* To whom correspondence should be addressed. Telephone: (614) 688-4068. Fax: (614) 292-1532. E-mail: pei.3@osu.edu.

[1] Abbreviations: Cinn-GEE, *N*-[4-(3-oxo-1-propenyl)benzoyl]-Gly-Glu-Glu-NH_2; Cinn-ARL, *N*-{2-[4-(3-oxo-1-propenyl)phenoxy]acetyl}-Ala-Arg-Leu-NH_2; HSQC, heteronuclear single-quantum coherence; PTP, protein tyrosine phosphatase; PTK, protein tyrosine kinase; pY, phosphotyrosine; *p*NPP, *p*-nitrophenyl phosphate; SH2, Src homology 2.

10.1021/bi034076u CCC: $25.00
Published on Web 04/11/2003

SH2 inhibitors contain negatively charged phosphonates (*13*−*16*) or carboxylates (*17*−*21*) as pY isosteres, which adversely affect their membrane permeability. We report here that peptidyl aldehydes can act as covalent inhibitors of SH2 domains derived from protein tyrosine phosphatase SHP-1 (*22*). This finding should open the door to a new family of neutral pY mimetics, which have much better membrane permeability and can potentially overcome the second challenge in designing SH2 domain inhibitors.

MATERIALS AND METHODS

Materials and General Methods. SHP-1, its catalytic domain [SHP-1(ΔSH2)], and the R30K mutant were purified from a recombinant *Escherichia coli* strain as previously described (*23*, *24*). The N- and C-terminal SH2 domains, either as their maltose-binding protein (MBP) or glutathione *S*-transferase (GST) fusion proteins or as C-terminal histidine-tagged proteins, were expressed and purified as previously described (*25*). All of the peptide synthesis reagents were purchased from Advanced ChemTech (Louisville, KY). The Rink resin had a loading capacity of 0.7 mmol/g. All other chemicals were obtained from Aldrich or Sigma.

*tert-Butyl 2-(4-Formylphenoxy)acetate (**5**)*. NaH (0.26 g, 11 mmol) was added to a solution of 4-hydroxybenzaldehyde (1.22 g, 10 mmol) in 20 mL of DMF at room temperature, and the resulting mixture was stirred for 30 min under argon. $BrCH_2COOtBu$ (1.95 g, 10 mmol) was then added to the above solution, and the reaction was continued for 1 h at 80 °C. After cooling, the reaction mixture was partitioned between ethyl acetate and water. The organic layer was sequentially washed with 1 M aqueous NaOH and water, dried over anhydrous $MgSO_4$, and evaporated to an oil, which was subsequently purified by silica gel chromatography (4:1 hexane/ethyl acetate) (yield 1.56 g or 66%). ^{1}H NMR (250 MHz, $CDCl_3$): 9.89 (s, 1H, CHO), 7.88 (d, 2H, J = 13.2 Hz, Ar), 7.00 (d, 2H, J = 13.2 Hz, Ar), 4.59 (s, 2H, OCH_2-CO), 1.51 (s, 9H, tBu). ^{13}C NMR: 190.74, 167.15, 162.77, 131.93, 130.56, 114.85, 82.91, 65.51, 27.79.

*tert-Butyl 2-{4-[2-(1,3-Dioxolan-2-yl)ethenyl]phenoxy}-acetate (**6**)*. Compound **5** (1.56 g, 6.6 mmol) and tris[2-(2-methoxyethoxy)ethyl]amine (TDA-1) (2.14 g, 6.6 mmol) were dissolved in dichloromethane (40 mL) under argon at room temperature. A saturated aqueous K_2CO_3 solution (40 mL) and (1,3-dioxolan-2-ylmethyl)triphenylphosphonium bromide (2.85 g, 6.6 mmol) were added, and the reaction mixture was refluxed at 40 °C for 18 h with vigorous stirring. The reaction mixture was extracted with dichloromethane (2 × 20 mL), washed with water (15 mL), and dried over $MgSO_4$. Compound **6** was obtained as a mixture of *E* and *Z* isomers (yield 1.77 g, 87.6%). ^{1}H NMR (250 MHz, $CDCl_3$): 7.26−7.36 (m, 2H, Ar), 6.83−6.89 (m, 2H, Ar), 6.72−6.76 (2 d, 1H, ArC*H* *E* and *Z*), 6.01 (dd, 0.41 H, ArCHC*H*CH *E*, J = 5.7 and 15.8 Hz), 5.65 (dd, 0.59 H, ArCHC*H*CH *Z*, J = 7.3 and 11.8 Hz), 5.52 (d, 0.59 H, ArCHCHC*H* *Z*, J = 7.3 Hz), 5.41 (d, 0.41 H, ArCHCHC*H* *E*, J = 5.7 Hz), 4.51 (s, 2H, OCH_2CO), 3.92−4.08 (m, 4H, OCH_2CH_2O), 1.49 (s, 9H, tBu).

*Ethyl 2-{4-[2-(1,3-Dioxolan-2-yl)ethenyl]phenoxy}acetyl Carbonate (**7**)*. An aqueous NaOH solution (0.93 g dissolved in 6 mL of water) was added to compound **6** (1.77 g, 5.8 mmol) dissolved in 10 mL of methanol. The solution was refluxed for 8 h until the ester is completely hydrolyzed, and the solvent was removed by rotary evaporation. The residue was dried over P_2O_5 in vacuo to afford a white solid. The solid was suspended in 25 mL of dichloromethane, and ethyl chloroformate (3.78 g) was added. The mixture was stirred for 40 min at room temperature and filtered. The filtrate was evaporated under reduced pressure to produce **7** as a 4:1 mixture of *Z* and *E* isomers (yield 1.35 g, 72.4%). ^{1}H NMR (250 MHz, $CDCl_3$): δ 7.32−7.36 (m, 2H, Ar), 6.89−6.92 (m, 2H, Ar), 6.72−6.77 (2 d, 1H, ArC*H* *E* and *Z*), 6.06 (dd, 0.21 H, ArCHC*H*CH *E*, J = 5.6 and 15.7 Hz), 5.64 (dd, 0.79 H, ArCHC*H*CH *Z*, J = 7.4 and 11.8 Hz), 5.48 (d, 0.79 H, ArCHCHC*H* *Z*, J = 7.4 Hz), 5.38 (d, 0.21 H, ArCHCHC*H* *E*, J = 5.6 Hz), 4.76 (2 s, 2H, OCH_2CO *Z* and *E*), 4.32−4.41 (m, 2H, OCH_2CH_3), 3.81−4.08 (m, 4H, OCH_2CH_2O), 1.30−1.41 (t, 3H, OCH_2CH_3).

*N-{2-[4-(3-Oxo-1-propenyl)phenoxy]acetyl}-Ala-Arg-Leu-NH$_2$ (**1**)*. The tripeptide Ala-Arg-Leu was synthesized on 0.15 g of Rink resin (0.10 mmol) using standard Fmoc/HBTU/HOBt solid-phase chemistry. Next, 64 mg (0.20 mmol) of anhydride **7** in 2.5 mL of dichloromethane and 100 μL of *N*-methylmorpholine were added to the resin suspended in 2.5 mL of anhydrous DMF. The mixture was shaken for 8 h at room temperature. Ninhydrin tests indicated complete acylation of the N-terminal amine. The solvents were drained, and the resin was washed with DMF (5 × 5 mL) and methanol (3 × 5 mL). Deprotection of side chains as well as the aldehyde protecting group and cleavage from the resin were carried out with a cocktail containing 4 mL of 90% TFA in water, 0.1 mL of anisole, and 0.15 mL of thioanisole for 3 h at room temperature. After removal of the volatile chemicals by a gentle flow of nitrogen, the residue was triturated five times with diethyl ether. Compound **1** was obtained as a brownish solid in the pure *E* isomer form. HPLC analysis showed a single major peak of at least 80% purity (monitored at 291 nm, which is the λ_{max} of the cinnamaldehyde group). HRESI-MS: $C_{26}H_{40}N_7O_6^+$, calcd 546.3035, found 546.3122.

*N-[4-(3-Oxo-1-propenyl)benzoyl]-Gly-Glu-Glu-NH$_2$ (**2**) and N-[4-(3-[^{13}C]Oxo-1-propenyl)benzoyl]-Gly-Glu-Glu-NH$_2$ (**10**)*. These compounds were synthesized as previously described (*26*).

*4-(3-Oxo-1-propenyl)benzoic Acid (**3**) and Ethyl 4-[2-(1,3-Dioxolan-2-yl)ethenyl]benzoyl Carbonate (**9**)*. These compounds were synthesized as previously described (*26*).

*N-[4-(3-Oxo-1-propenyl)benzoyl]-Gly-Glu-Glu-βAla-βAla-βAla-(N$^\epsilon$-Biotinyl)Lys-NH$_2$ (**4**)*. The unbiotinylated precursor of this compound was synthesized from anhydride **9** on the solid phase in a manner similar to compound **1**. The fully deprotected compound (1.8 mg, 1.6 μmol) containing a single amino group on the lysyl residue was dissolved in 1 mL of 30 mM Na_2HPO_4 (pH 9.2), and *N*-hydroxysuccinimidobiotin (0.5 μmol) in 10 μL of DMF was added. The mixture was incubated at room temperature for 2.5 h. The use of a substoichiometric amount of the biotinylating agent was to avoid binding to the streptavidin sensorchip (see below) by free biotin. HPLC analysis showed an approximately 50:50 mixture of biotinylated and unbiotinylated peptides, which was essentially free of other species when monitored at 291 nm. ESI-MS: $C_{47}H_{68}N_{11}O_{15}S^+$, calcd 1058.4601, found 1058.4.

Activation of SHP-1 by Peptidyl Aldehydes. Phosphatase activity of SHP-1 was measured with *p*-nitrophenyl phosphate (*p*NPP) as substrate. The assay reaction (total volume of 50 μL) contained 50 mM Hepes, pH 7.4, 50 mM NaCl, 1 mM EDTA, 1 mM tris(carboxyethyl)phosphine, 10 mM *p*NPP, 0−2000 μM peptidyl aldehyde (or other effectors), and 0.5 μg of SHP-1. The reaction was initiated by the addition of SHP-1 as the last component and allowed to proceed at room temperature (~23 °C) for 30 min. The reaction was then quenched with 950 μL of 1 M NaOH, and the absorbance at 405 nm was measured on a Perkin-Elmer UV−vis spectrophotometer. The SHP-1 reactivity reported was relative to that of SHP-1 in the absence of any SH2 inhibitor. The time−course experiment was carried out under similar conditions except that the reaction (total volume of 1.0 mL) contained 45 μM Cinn-GEE and 10 μg of SHP-1. To demonstrate the reversibility of the interaction, SHP-1 (1.0 μg) was incubated with 0 or 600 μM Cinn-GEE in the above buffer (10 μL) for 3 min. The resulting mixture was rapidly diluted into 990 μL of the same buffer containing 10 mM *p*NPP, and the reaction was monitored at 405 nm on the spectrophotometer.

SH2 Domain−Inhibitor Binding Assays. Surface plasmon resonance measurements were carried out on a Pharmacia BIAcore 3000 instrument. A biosensorchip containing immobilized streptavidin was conditioned with 1 M NaCl in 50 mM NaOH according to manufacturer's instructions. The biotinylated Cinn-GEE (compound **4**) was immobilized onto the biosensorchip by flowing a 0.8 μM solution of **4** for 8 s (flow rate = 15 μL/min). Increasing concentrations of the GST-SH2(N) protein (0−15 μM) in HBS-EP buffer (10 mM Hepes, pH 7.4, 150 mM NaCl, 3 mM EDTA, and 0.005% polysorbate 20) was allowed to flow over the sensorchip for 10 min at a flow rate of 15 μL/min. A blank flow cell (no compound **4**) was used as the control to correct for any signal due to the solvent bulk and/or nonspecific binding interactions. In between two runs, the chip surface was regenerated by flowing 0.05% SDS in HBS-EP buffer for 10 s at a flow rate of 30 μL/min. Data analysis was carried out by plotting the equilibrium response units (RU_{eq}), obtained by subtracting the response of the blank flow cell from that of the Cinn-GEE immobilized flow cell, against the SH2 protein concentration. The dissociation constant (K_D) was obtained by fitting the data to the equation

$$RU_{eq} = RU_{max}[SH2]/(K_D + [SH2])$$

where RU_{eq} is the measured response unit at a certain SH2 concentration and RU_{max} is the maximum response possible. Binding of the C-SH2 domain was carried out similarly, except that higher SH2 protein concentrations were used (5−50 μM) and the C-SH2 domain contained a C-terminal histidine tag.

For competition experiments, a biotinylated pY peptide, biotin-A(β-Ala)$_3$IYpYANLI, was immobilized onto streptavidin-coated sensorchip SA as previously described (*25*). GST-SH2(N) protein (10 μM) was preincubated with/without Cinn-GEE (300 μM) for 10 min at room temperature and passed over the sensorchip for 3 min at a flow rate of 15 μL/min. A blank flow cell was used as a control to correct any signal generated due to the solvent bulk or nonspecific interactions.

NMR Spectroscopy of [^{13}C]Cinn-GEE and the [^{13}C]Cinn-GEE−SH2 Complex. All NMR experiments were performed for 6−12 h on a Bruker DMX-600 NMR spectrometer equipped with a triple-resonance and three-axes gradient probe at 300 K. The 2D ^{1}H−^{13}C heteronuclear single-quantum coherence spectra (HSQC) were acquired using a constant-time sensitivity-enhanced method (*27*, *28*). The N-SH2 domain used was a fusion protein with maltose-binding protein [MBP-SH2(N)], whereas the C-terminal SH2 domain contained a C-terminal histidine tag. All samples were dissolved in a buffer containing 5 mM Hepes (pH 7.4), 100 mM NaCl, 1 mM EDTA, and 1 mM β-mercaptoethanol (94:6 H_2O/D_2O). The samples were incubated at room temperature for 30 min prior to NMR experiments. The spectral widths were 9615 Hz in the ^{1}H dimension and 19621 Hz in the ^{13}C dimension, with carrier frequencies at 4.7 and 150 (for ^{13}C at the aldehyde position), respectively.

Mass Spectrometry. MBP-SH2(N) (100 μM) was incubated with [^{13}C]Cinn-GEE (140 μM) for 30 min in a buffer containing 10 mM Hepes (pH = 7.4), 150 mM NaCl, 3 mM EDTA, and 1 mM β-mercaptoethanol. After that, 1 μL of 200 mM sodium cyanoborohydride in water was added each hour for a total of 5 h. The resulting mixture was incubated for an additional 16 h. Prior to MS analysis, the mixture was dialyzed against a 30 mM ammonium acetate buffer for 12 h. Electrospray ionization (ESI) experiments were performed on a Micromass Q-Tof II (Micromass, Wythenshawe, U.K.) mass spectrometer equipped with an orthogonal electrospray source (Z-spray) operated in the positive ion mode. Sodium iodide was used for mass calibration for a calibration range of *m*/*z* 100−2500. Salt buffers from the protein samples were cleaned using manual syringe protein traps from Michrom BioResources (Auburn, CA). Proteins were prepared in a solution containing 50% acetonitrile/50% water and 0.1% formic acid at a concentration of 10 pmol/μL and infused into the electrospray source at a rate of 5−10 μL/min. Optimal ESI conditions were as follows: capillary voltage, 3000 V; source temperature, 110 °C; cone voltage, 60 V. The ESI gas was nitrogen. Q1 was set to optimally pass ions from *m*/*z* 500−1990, and all ions transmitted into the pusher region of the TOF analyzer were scanned over *m*/*z* 500−3000 with a 1 s integration time. Data were acquired in the continuum mode until acceptable averaged data were obtained (10−15 min). ESI data were deconvoluted using MaxEnt I provided by Micromass. A control experiment was carried out similarly except that no sodium cyanoborohydride was added.

RESULTS

Stimulation of SHP-1 Activity by Peptidyl Aldehydes. We have recently reported that peptidyl aldehydes act as slow-binding inhibitors of PTPs (*26*). They bind to the PTP active site as a pY mimetic to form an initial noncovalent complex, E·I, which is slowly converted into a covalent enamine adduct (E·I*) with an active site arginine (Arg-221 in PTP1B). Arg-221 is a universally conserved residue among PTPs and is critical for pY substrate binding as well as transition-state stabilization by forming a pair of hydrogen bonds between the phosphate oxygen atoms and the guanidinium group (*29*, *30*). This finding led us to hypothesize that the aldehydes may also act as SH2 domain antagonists. Both PTPs and SH2 domains recognize pY peptides as their

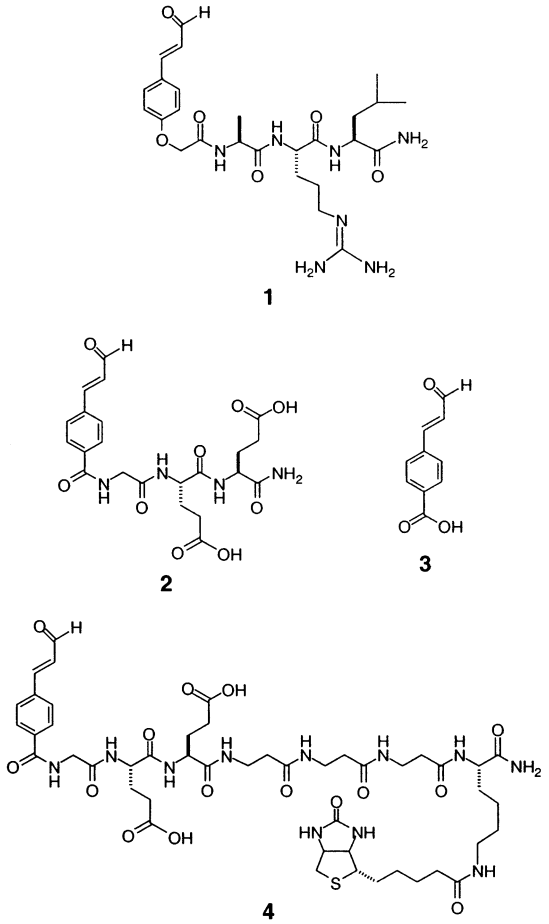

FIGURE 1: Structures of PTP inhibitors.

Scheme 1

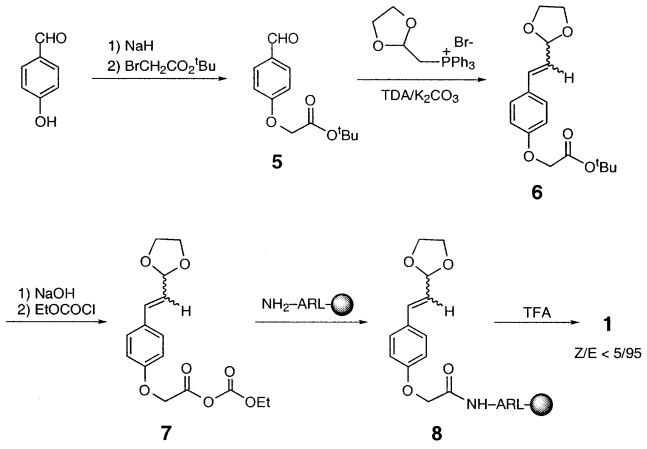

natural ligands, and their active/binding sites have remarkable similarities. Like PTPs, SH2 domains utilize the guanidinium group of an absolutely conserved arginine (Arg βB5) to form a pair of hydrogen bonds with the phosphate group of pY (*6*−*9*). A key difference is that the SH2 domains lack the catalytic cysteine in the PTP active site.

To test the above notion, we synthesized a peptidyl aldehyde, *N*-{2-[4-(3-oxo-1-propenyl)phenoxy]acetyl}-Ala-Arg-Leu (Cinn-ARL) (compound **1** in Figure 1) (Scheme 1). Our previous study showed that pY peptides of the consensus LXpYARLI (X = any amino acid) bind to both N- and C-SH2 domains of SHP-1 with high affinity (*25*). We employed Cinn-ARL to stimulate the phosphatase

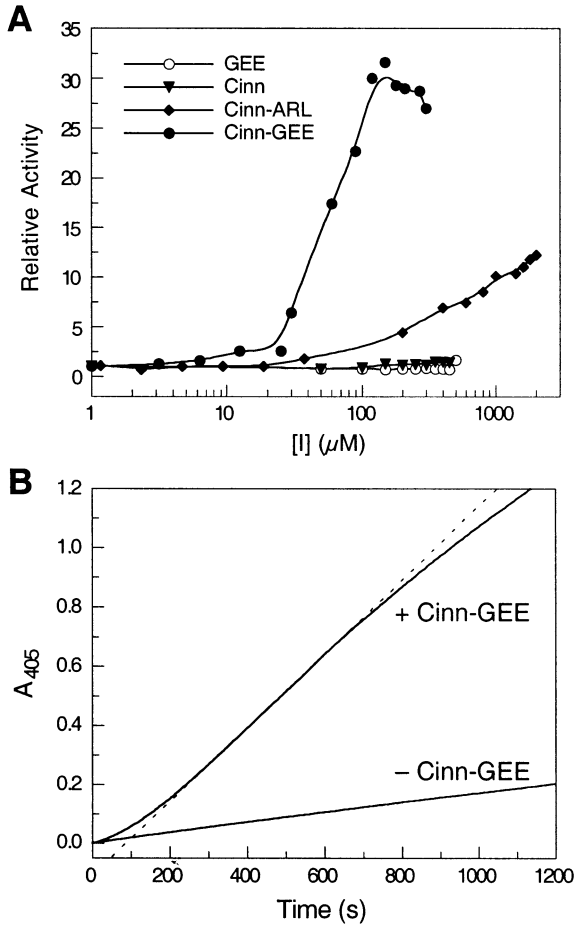

FIGURE 2: Activation of SHP-1 by peptidyl aldehydes. (A) Plot of SHP-1 activity against SH2 domain inhibitor concentration. The data presented are phosphatase activities relative to that of SHP-1 in the absence of peptidyl aldehyde. (B) Time course of the activation of SHP-1 by Cinn-GEE. The reaction was initiated by the addition of SHP-1 (0.15 μM final concentration) to a solution containing the reaction buffer (pH 7.4), 10 mM *p*NPP, and 0 or 45 μM Cinn-GEE and monitored continuously at 405 nm on a UV−vis spectrophotometer. The dashed straight line is drawn for comparison.

activity of SHP-1 as a convenient test of its ability to bind the N-SH2 of SHP-1. Under physiological conditions, SHP-1 exists as an inactive form, in which the N-SH2 directly binds to and inactivates the PTP domain (*24*, *31*). Binding of a high-affinity ligand (e.g., a pY peptide) to the N-SH2 disrupts the SH2−PTP interaction and increases its activity by up to 30-fold. As shown in Figure 2A, Cinn-ARL stimulated SHP-1 activity by up to 13-fold, with half-maximal activation (IC_{50}) reached at ~500 μM. Assuming an equilibrium constant of ~30 between the open and closed states of SHP-1 (*24*, *31*), we estimated a dissociation constant (K_D) of ~17 μM for the interaction between Cinn-ARL and the isolated N-SH2 domain. Under the assay conditions, Cinn-ARL showed no significant inhibition toward the catalytic domain of SHP-1, SHP-1(ΔSH2) (*23*), up to 1 mM inhibitor concentration (data not shown). As a control, we also tested *N*-[4-(3-oxo-1-propenyl)benzoyl]-Gly-Glu-Glu (Cinn-GEE) (compound **2** in Figure 1), which had previously been shown as a fairly potent slow-binding inhibitor of PTP1B and SHP-1(ΔSH2) (K_I^* = 5.4 and 11 μM, respectively) (*26*). Surprisingly, Cinn-GEE is an even more potent activator of SHP-1 (with a maximum of ~30-fold stimulation) (Figure 2A).

Activation of SHP-1 by Cinn-GEE is dose-dependent, with maximal activity reached at 150 μM and half-maximal activity at ~60 μM. Further increase in Cinn-GEE concentration resulted in decreased PTP activity, due to inhibition of the PTP active site. Neither the tripeptide Gly-Glu-Glu nor cinnamaldehyde (**3**) alone showed significant stimulation of SHP-1 activity (<2-fold). The IC_{50} value suggests a K_D of ~2 μM for the Cinn-GEE−N-SH2 complex.

Given the K_I* value previously determined for SHP-1(ΔSH2) (11 μM), one would have expected that the PTP active site of SHP-1 be completely inhibited by 150 μM Cinn-GEE. A possible explanation for this apparent paradox is that the formation of the SH2−Cinn-GEE complex is much faster than that of the PTP−Cinn-GEE complex. Consequently, there is no significant amount of E·I* complex (i.e., the enamine adduct) formed between the PTP active site and Cinn-GEE during the 30 min activation assay period. To test this notion, we added SHP-1 into an assay solution containing reaction buffer, *p*NPP (10 mM), and Cinn-GEE (45 μM) and monitored product formation at 405 nm as a function of time. The reaction progress curve has a sigmoidal shape, composed of an early delay region (<200 s) and a linear region (200−700 s), followed by a tailing-off region (>700 s) (Figure 2B). The delay in the early region indicates that activation of SHP-1 (and thus binding of Cinn-GEE to the N-SH2 domain) is also time-dependent, as would be expected from a slow-binding mechanism similar to that of inhibition of PTPs (see Discussion). However, the onset of the linear phase at ~200 s suggests that formation of the final SH2−Cinn-GEE complex is essentially complete within 3 min for the N-SH2 domain (at 45 μM Cinn-GEE). Under similar conditions, formation of the E·I* complex between PTP and Cinn-GEE typically takes >10 min (*26*). Therefore, the linear region represents a period during which SHP-1 activation is already complete whereas no significant amount of the covalent PTP−Cinn-GEE complex is yet formed. Finally, the rate of *p*NPP hydrolysis tails off as an increasing amount of PTP is inactivated by Cinn-GEE. The control reaction in the absence of Cinn-GEE produced a straight line during the entire reaction time.

Direct Binding between Cinn-GEE and SH2 Domains. Cinn-GEE was tested for binding to the isolated N- and C-SH2 domains of SHP-1 using the surface plasmon resonance technique (BIAcore). Immobilization of the aldehyde ligand onto streptavidin-coated sensorchips was effected by the addition of a biotin to the C-terminus of Cinn-GEE. To maximize the accessibility of the surface-bound ligand to an incoming SH2 domain, a flexible linker of β-Ala-β-Ala-β-Ala-Lys (BBBK) was added to the C-terminus of Cinn-GEE. The resulting ligand was synthesized by solid-phase chemistry, deprotected, and treated with *N*-hydroxysuccinimidobiotin to give compound **4** (Figure 1). For binding studies, we employed the N-SH2 domain as a fusion protein with glutathione *S*-transferase [GST-SH2(N)], because the N-SH2 alone was not stable. The C-SH2 domain contained a C-terminal histidine tag. Figure 3A shows the sensorgrams for the binding of GST-SH2(N) to the immobilized Cinn-GEE, after correction for nonspecific binding to the surface. The slow increase in response units over several minutes (after the initiation of sample injection) even at saturating concentrations of the SH2 protein confirms that the interaction is slow binding in nature. In contrast, binding

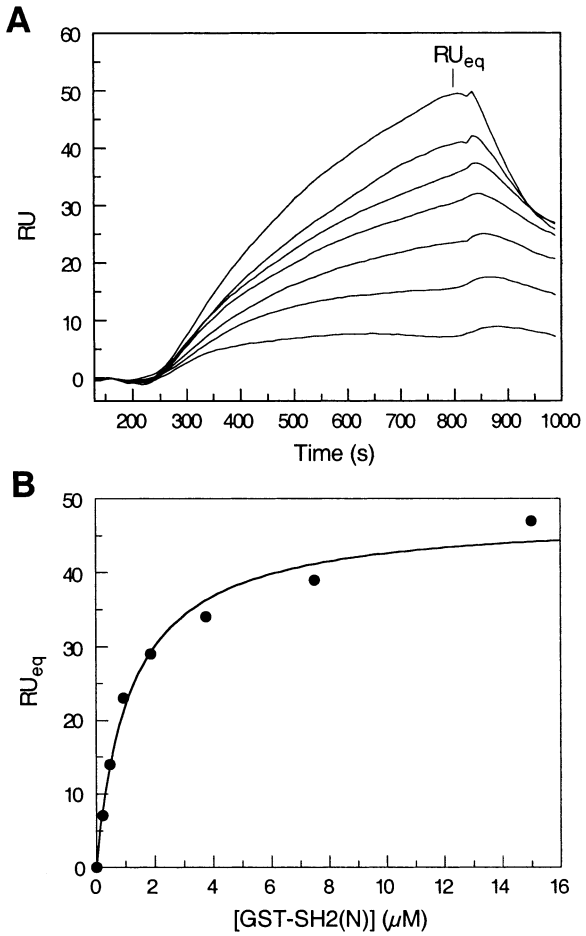

FIGURE 3: BIAcore analysis of the binding of GST-SH2(N) to immobilized Cinn-GEE (*4*). (A) Overlaid sensorgrams at increasing concentrations of GST-SH2(N) (0.23, 0.47, 0.94, 1.87, 3.75, 7.50, and 15 μM). (B) Plot of resonance signal under equilibrium binding conditions (signal difference between the points immediately before the initiation and at the end of each injection) against SH2 concentration. Data were fitted to the equation $RU_{eq} = RU_{max}[SH2]/(K_D + [SH2])$.

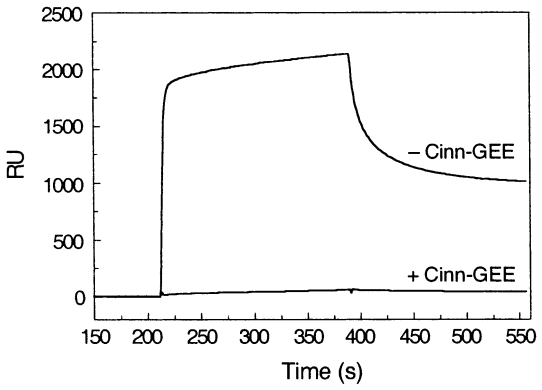

FIGURE 4: Competition of Cinn-GEE and peptide IYpYANLI for binding to GST-SH2(N). The pY peptide was immobilized onto a streptavidin-coated BIAcore sensorchip as previously described (*24*). GST-SH2(N) (10 μM) was allowed to flow over the surface in the absence or presence of Cinn-GEE (300 μM).

of GST-SH2(N) to immobilized pY peptides displays rapid kinetics (refs *24* and *25* and Figure 4). A plot of equilibrium response units (RU_{eq} = difference in response units prior to and at the end of sample injection) against SH2 concentration clearly showed saturation behavior, and data fitting gave an equilibrium K_D of 1.3 ± 0.2 μM (Figure 3B). This value is

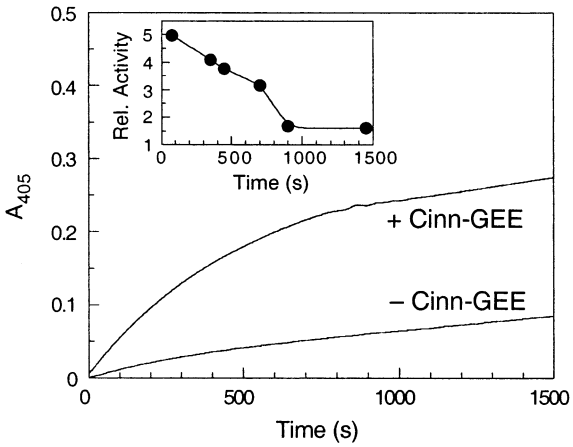

FIGURE 5: Time-dependent dissociation of the Cinn-GEE−SH2 domain complex. SHP-1 (1.5 μM) was preincubated with 0 or 600 μM Cinn-GEE for 3 min before being diluted 100-fold into an assay buffer containing 10 mM *p*NPP. The reaction progress curves as monitored at 405 nm are shown. Inset, the relative rate of *p*NPP hydrolysis (the ratio of reaction rate in the presence of Cinn-GEE over control) as a function of time.

similar to the K_D value (~2 μM) estimated from the SHP-1 activation profile. The C-SH2 domain also bound to the immobilized Cinn-GEE with an estimated K_D of ~25 μM (the K_D value could not be accurately determined due to significant nonspecific binding at high SH2 protein concentrations).

Cinn-GEE Is Active Site Directed. To determine whether Cinn-GEE binds to the canonical pY-binding site of the SH2 domains, competition experiments were performed with a pY peptide, IYpYANLI, which binds to the N-SH2 domain of SHP-1 with high affinity (K_D = 0.6 μM) (*25*). As shown in Figure 4, GST-SH2(N) protein alone (10 μM) bound very well to a sensorchip immobilized with the pY peptide. However, preincubation of the N-SH2 domain (10 μM) with excess Cinn-GEE (300 μM) completely abolished its binding to the sensorchip, under otherwise identical conditions. In a reverse competition experiment, the pY peptide also inhibited the binding of GST-SH2(N) to the immobilized Cinn-GEE (data not shown). These results indicate that Cinn-GEE and IYpYANLI bind to the same site on the SH2 domain.

Cinn-GEE−SH2 Domain Interaction Is Reversible. The fact that a pY peptide can displace GST-SH2(N) bound to the immobilized Cinn-GEE indicates that the interaction between Cinn-GEE and the SH2 domain is reversible. To further demonstrate the reversibility of the interaction, SHP-1 was preincubated with excess Cinn-GEE to form the Cinn-GEE−SH2 domain complex, which was then rapidly diluted into an assay solution containing *p*NPP as substrate. The reaction progress as a function of time is shown in Figure 5. Initially, the rate of *p*NPP hydrolysis (as indicated by the slope at time 0) was relatively high; as time increased, the reaction rate decreased, eventually approaching the rate of *p*NPP hydrolysis by SHP-1 in the absence of Cinn-GEE. The simplest explanation is that, at time 0, the N-SH2 domain was occupied by Cinn-GEE and SHP-1 was in the active form, whereas dilution caused time-dependent dissociation of the Cinn-GEE−SH2 domain complex and re-formation of the catalytically inactive SH2−PTP complex. Due to the complication of simultaneous inhibition of the PTP active site by Cinn-GEE, we have not been able to determine quantitatively the kinetics of Cinn-GEE−SH2 dissociation.

Mechanism of the Cinn-GEE−SH2 Domain Interaction. To determine the mechanism by which Cinn-GEE binds the SH2 domains, we synthesized Cinn-GEE labeled with ^{13}C at the aldehyde carbonyl carbon and analyzed both the inhibitor (compound **10**) and the SH2 domain−inhibitor complexes by $^{1}H-^{13}C$ HSQC NMR spectroscopy. When dissolved in the assay buffer (pH 7.4), [^{13}C]Cinn-GEE alone showed a single cross-peak at δ 9.64 (^{1}H) and δ 201 (^{13}C) in the NMR spectrum (Figure 6A). This suggests that the free inhibitor existed predominantly in the aldehyde form in the aqueous solution. Addition of excess N-SH2 domain (with preincubation) resulted in the disappearance of the free inhibitor signal, with concomitant appearance of a new cross-peak at δ 8.45/173 (Figure 6B). No other signals were observed that could be attributed to either the free inhibitor or the enzyme−inhibitor complex. The large change in

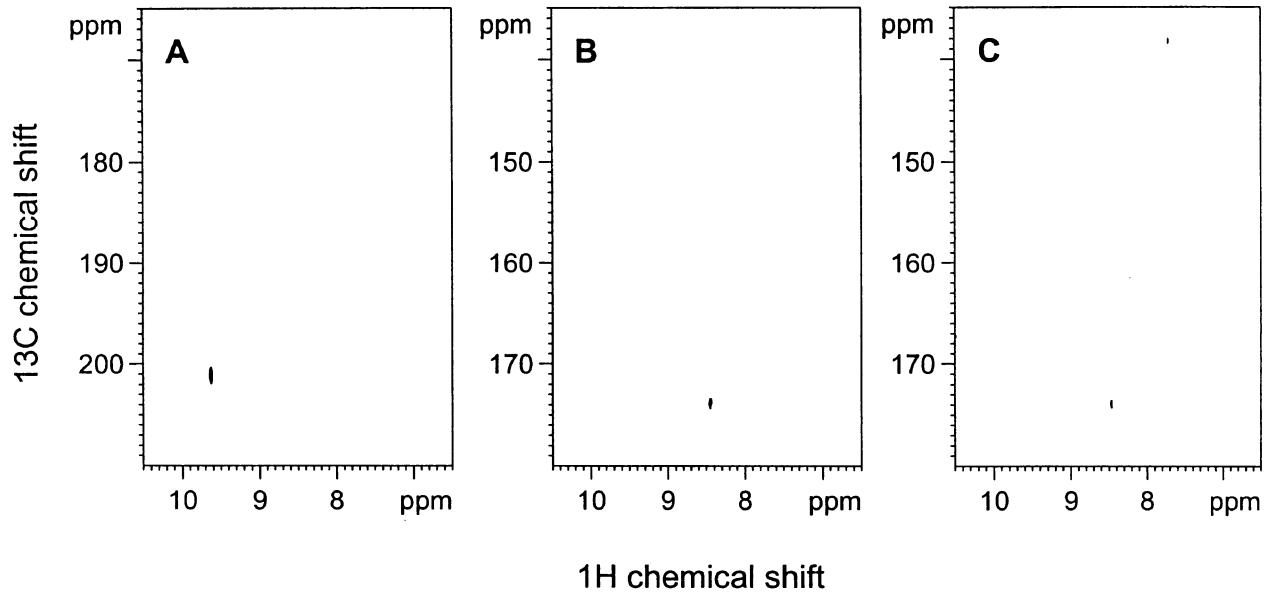

FIGURE 6: HSQC spectra of ^{13}C-labeled Cinn-GEE in the presence and absence of SH2 protein: (A) 200 μM Cinn-GEE only; (B) 200 μM Cinn-GEE and 400 μM N-SH2 domain; (C) 200 μM Cinn-GEE and 400 μM C-SH2 domain.

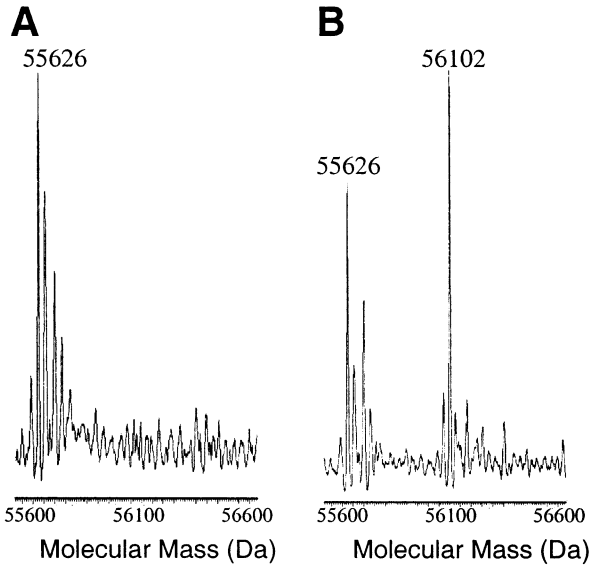

FIGURE 7: Deconvoluted spectra from LC-ESI MS analyses of the [^{13}C]Cinn-GEE−MBP-SH2(N) complex before (A) and after treatment with sodium cyanoborohydride (B).

chemical shift values upon binding suggests that the inhibitor underwent covalent interaction with a single group in the SH2 domain. Furthermore, the chemical shift value (δ 173 for ^{13}C) suggests that the labeled carbon atom is still in the sp^2 hybridization state in the covalent SH2−inhibitor complex. The HSQC spectrum for the C-SH2 domain−Cinn-GEE complex is somewhat more complex; in addition to a cross-peak at δ 8.45/174, it has a second cross-peak of slightly lower intensity at δ 7.70/139 (Figure 6C). The chemical shift values of the latter peak are very similar to those observed for the enamine adduct formed between Cinn-GEE and the active site arginine of PTP1B (*26*). These observations, as well as the precedence of PTP1B−Cinn-GEE interaction, led us to propose that Cinn-GEE binds to the N-SH2 domain by forming an imine adduct with an active site arginine (most likely Arg βB5), whereas the C-SH2 domain forms a mixture of imine and enamine adducts.

To gain further evidence for the proposed mechanism, we attempted to analyze the N-SH2 domain−Cinn-GEE complex by mass spectrometry. However, we have so far failed to observe the covalent adduct directly, probably due to the reversible nature of the adduct and the moderate affinity (K_D = 1.3 μM). We next incubated the N-SH2 domain with Cinn-GEE under the same conditions but in the presence of a reducing agent, sodium cyanoborohydride. ESI-MS analysis of the reaction mixture revealed a new species with a molecular mass of 56102 ± 5 Da in the spectrum, in addition to the unmodified MBP-SH2(N) protein (molecular mass = 55626 ± 5 Da) (Figure 7). The difference in molecular mass between the peaks was ~476 Da, suggesting the addition of a single inhibitor molecule to the protein (491 − 18 + 2 = 475 Da). No peak corresponding to the addition of two or more inhibitors to the SH2 domain was observed. These results are consistent with the formation of a reversible imine adduct between Cinn-GEE and an amino group of the SH2 domain, which was reduced to a stable amine adduct by sodium cyanoborohydride. Unfortunately, all of our attempts to isolate and sequence a proteolytic fragment containing the covalently attached inhibitor have failed.

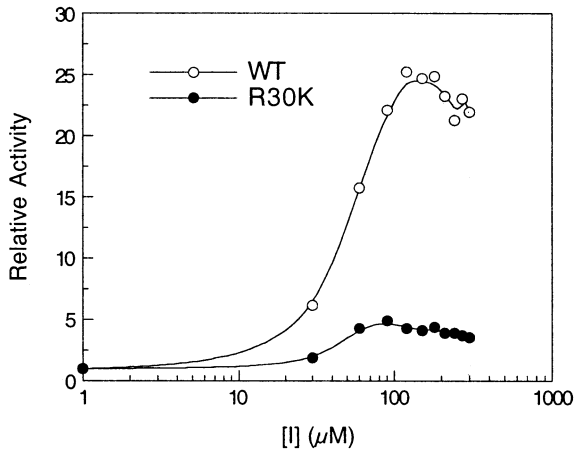

FIGURE 8: Comparison of the stimulatory effect of Cinn-GEE on wild-type and R30K SHP-1.

The role of Arg βB5 (Arg-30 in SHP-1) in inhibitor binding was assessed by constructing an R30K mutant of SHP-1 and examining its ability to be activated by Cinn-GEE. Unlike the wild-type enzyme, whose activity is stimulated by up to 25−30-fold by Cinn-GEE, the R30K enzyme is much less responsive to Cinn-GEE stimulation (<5-fold stimulation at maximum) (Figure 8). This shows that Arg-30 is intimately involved in inhibitor binding, most likely acting as the attacking nucleophile (see Discussion). A possible explanation for the weaker binding of Cinn-GEE to the R30K mutant SH2 domain is that the lysine side chain may be too short to reach the inhibitor aldehyde in the initial noncovalent complex.

DISCUSSION

We have shown that peptidyl aldehydes display slow-binding inhibition of SH2 domains derived from SHP-1. Although the SH2 domains have no catalytic activity, we will treat them as "enzyme entities (E)" in order to apply the kinetic models developed for enzymatic systems. Thus, the kinetics of SH2 inhibition can be described by the equation

$$E + I \overset{K_I}{\rightleftharpoons} E{\cdot}I \underset{k_6}{\overset{k_5}{\rightleftharpoons}} E{\cdot}I^*$$

where K_I is the equilibrium inhibition constant for the formation of the initial complex, E·I, and k_5 and k_6 are the forward and reverse rate constants for the slow conversion of the initial E·I complex into a tight complex, E·I*, respectively. The overall potency of the inhibitor is described by the overall equilibrium constant, $K_I^* = K_I k_6/(k_5 + k_6)$. Due to technical difficulties, we have not yet been able to determine the K_I, k_5, and k_6 values. However, the K_I^* value, which equals to the apparent dissociation constant (K_D) measured under equilibrium conditions, can be determined. Binding studies using surface plasmon resonance gave K_I^* (or K_D) values of 1.3 and ~25 μM for the binding of Cinn-GEE to the N- and C-SH2 domains, respectively. The former value agrees quite well with the K_D value (~2 μM) estimated from the SHP-1 activation profile. Therefore, the peptidyl aldehydes are fairly potent inhibitors of SH2 domains. We are confident that still more potent inhibitors can be developed by optimizing the peptide sequence or by attaching appropriate peptidomimetics to cinnamaldehyde.

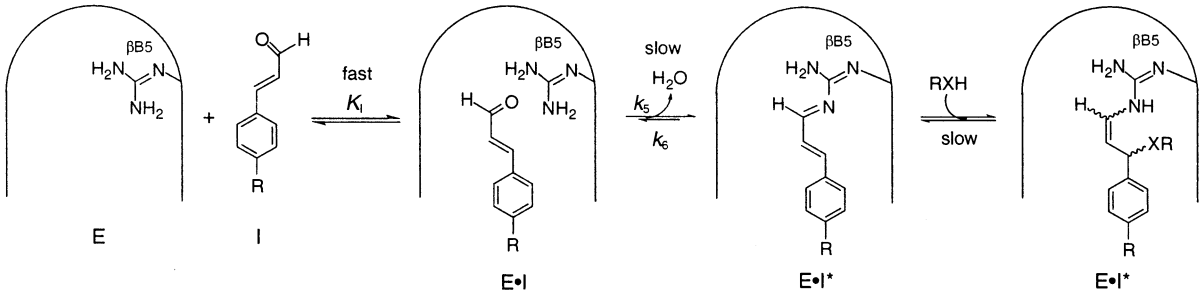

FIGURE 9: Proposed mechanism of inhibition of SH2 domains by peptidyl cinnamaldehyde derivatives. RXH, the yet unidentified nucleophile.

Figure 9 shows our proposed mechanism for the observed slow-binding inhibition. The cinnamaldehyde moiety binds to the pY-binding pocket to form the initial E·I complex, in which the aldehyde carbonyl group is placed in close proximity to the guanidine group of Arg βB5. Nucleophilic addition on the carbonyl by one of the guanidino amine groups followed by dehydration generates a conjugated imine adduct. The imine can be further converted into an enamine adduct (in the C-SH2 domain) through conjugate addition at the benzylic position by a yet unidentified nucleophile. This mechanism is very similar to that proposed for the inhibition of PTP1B by Cinn-GEE (*26*) and is consistent with all of the experimental observations. The chemical shift values for the aldehyde-derived proton/carbon in the E·I* complex (δ 8.45/~174 and δ 7.70/139) indicate that the aldehyde carbonyl is no longer present but the carbon atom is still sp^2 hybridized. This suggests that the aldehyde must have reacted with an active site residue to form an adduct involving a double bond at the carbonyl carbon. Further, the formation of this adduct must be reversible. Among the 20 proteinic amino acids, only lysine and arginine are capable of forming such a structure with an aldehyde (in the form of an imine or enamine). To determine which arginine or lysine residue is involved in the reaction, we modeled the structures of the N- and C-SH2 domains of SHP-1 based on the X-ray crystal structure of the N-terminal SH2 domain of SHP-2, which has ~60% sequence identity to SHP-1 (*8*). The results show that the pY-binding pocket of N-SH2 contains three arginine residues (at positions βB5, BC1, and βD6) and a lysine (at position BC2), whereas the C-SH2 domain contains only one arginine (at position βB5) and one lysine (at position βD6). Therefore, Arg βB5 is the only candidate that is common to both SH2 domains. Arg βB5 is similarly situated at the pY-binding pocket to Arg-221 in the active site of PTP1B, which has been established as the residue modified by Cinn-GEE (*26*). Like Arg-221, Arg βB5 also forms a pair of hydrogen bonds with the phosphate group of the bound pY (*6*−*9*). In contrast, the side chain of Lys βD6, the other candidate residue in the C-SH2 domain, is packed against the phenyl ring of bound pY and is more distant from the phosphate group (*8*). Furthermore, the minor cross-peak (δ 7.70/139) in the HSQC spectrum of the C-SH2−Cinn-GEE complex has very similar chemical shift values to those of the enamine adducts formed between Arg-221 and the inhibitor aldehyde in the PTP1B−Cinn-GEE complex (δ 7.6−7.8/130−137) (*26*). Finally, the reversible adduct can be reduced to a stable adduct by sodium cyanoborohydride, and the R30K mutation dramatically decreased the ability of the N-SH2 domain to bind Cinn-GEE. Collectively, these data make a compelling case that Arg βB5 is the residue modified by Cinn-GEE in both SH2 domains. Thus, we propose that the minor cross-peak at δ 7.70/139 (in the C-SH2 domain) represents the enamine adduct formed between the inhibitor and Arg βB5, whereas the major peak at δ 8.45/~174 (in both N- and C-SH2 domains) is the conjugated imine adduct (Figure 9).

The proposed mechanism provides a sensible account for the activation of SHP-1 by peptidyl aldehydes. It is well established that pY peptides with high affinity to the N-SH2 domain can disrupt the intramolecular complex between the N-SH2 domain and the PTP active site (*24*, *31*). This relieves the autoinhibition by the N-SH2 domain and results in increased PTP activity. The peptidyl aldehydes bind to the same site as the pY ligands and are therefore expected to have the same stimulatory effect. The initial lag period (Figure 2B) is also expected, since the formation of the SH2·I* complex is time-dependent and relatively slow. The lack of significant inhibition of the PTP active site during the activation assays is due to the still slower formation of the PTP·I* complex and substrate protection (10 mM *p*NPP). The peptidyl aldehydes presumably also bound to the C-SH2 domain during the activation assays. However, binding to the C-SH2 domain has no effect on the catalytic activity of SHP-1 (*31*).

An important issue in designing SH2 domain inhibitors is selectivity. Namely, will a peptidyl aldehyde designed for a given SH2 domain inhibit other SH2 domains or other enzymes such as PTPs? The preliminary data from this work suggest that it should be possible to develop selective SH2 inhibitors. First, high-affinity binding to an SH2 domain requires both the peptide and the cinnamaldehyde moieties, as neither component alone had significant effect on SHP-1 activity. Indeed, Cinn-ARL and Cinn-GEE have a ~10-fold difference in binding affinity to the N-SH2 domain. The reason for the unexpected high affinity of Cinn-GEE (relative to Cinn-ARL) is not yet clear. Given the specificity of the N-SH2 domain for pYAXL peptides, it is possible that the tripeptides GEE and ARL bind to different sites near the pY-binding pocket. Second, Cinn-GEE showed a 20-fold difference in binding affinity to the N- vs C-SH2 domains of SHP-1, even though the two SH2 domains have similar specificity toward pY peptides (*25*). Finally, while Cinn-ARL showed respectable affinity to the N-SH2 domain, it had no detectable inhibition of the PTP active site.

In conclusion, we have demonstrated that peptidyl aldehydes function as covalent but reversible inhibitors of SH2 domains. The slow-binding kinetics is caused by the time-dependent conversion of the initial noncovalent complex to a covalent imine/enamine adduct with the conserved arginine (βB5) in the pY-binding pocket. The peptidyl aldehydes

represent a novel class of neutral SH2 domain inhibitors, which should overcome the permeability problems associated with the existing SH2 inhibitors.

ACKNOWLEDGMENT

The authors thank Drs. Chunhua Yuan and Kari Green-Church of the Campus Chemical Instrument Center (Ohio State University) for excellent technical assistance in the HSQC NMR and MS experiments.

REFERENCES

1. Pawson, T., and Gish, G. D. (1992) *Cell 71*, 359−362.
2. Bork, P., Schultz, J., and Ponting, C. P. (1997) *Trends Biochem. Sci. 22*, 296−298.
3. Venter, J. C., Adams, M. D., Myers, E. W., Li, P. W., Mural, R. J., Sutton, G. G., et al. (2001) *Science 291*, 1304−1351.
4. Songyang, Z., Shoelson, S. E., Chaudhuri, M., Gish, G., Pawson, T., Haser, W. G., King, F., Roberts, T., Ratnofsky, S., Lechleider, R. J., Neel, B. G., Birge, R. B., Fajardo, J. E., Chou, M. M., Hanafusa, H., Schaffhausen, B., and Cantley, L. C. (1993) *Cell 72*, 767−778.
5. Songyang, Z., Shoelson, S. E., McGlade, J., Oliver, P., Pawson, T., Bustelo, X. R., Barbacid, M., Sabe, H., Hanafusa, H., Yi, T., Ren, R., Baltimore, D., Ratnofsky, S., Feldman, R. A., and Cantley, L. C. (1994) *Mol. Cell. Biol. 14*, 2777−2785.
6. Waksman, G., Kominos, D., Robertson, S. C., Pant, N., Baltimore, D., Birge, R. B., Cowburn, D., Hanafusa, H., Mayer, B. J., Overduin, M., Resh, M. D., Rios, C. B., Silverman, L., and Kuriyan, J. (1992) *Nature 358*, 646−653.
7. Eck, M. J., Atwell, S. K., Shoelson, S. E., and Harrison, S. C. (1994) *Nature 368*, 764−769.
8. Lee, C.-H., Kominos, D., Jacques, S., Margolis, B., Schlessinger, J., Shoelson, S. E., and Kuriyan, J. (1994) *Structure 2*, 423−438.
9. Tong, L., Warren, T. C., King, J., Betageri, R., Rose, J., and Jakes, S. (1996) *J. Mol. Biol. 256*, 601−610.
10. Sawyer, T. K. (1998) *Biopolymers 47*, 243−261.
11. Shakespeare, W. C. (2001) *Curr. Opin. Chem. Biol. 5*, 409−415.
12. Shakespeare, W. C., Yang, M., Bohacek, R., Cerasoli, F., Stebbins, K., Sundaramoorthi, R., and Sawyer, T. (2000) *Proc. Natl. Acad. Sci. U.S.A. 97*, 9373−9378.
13. Burke, T. R., Jr., Smyth, M. S., Otaka, A., Nomizu, M., Roller, P. P., Wolf, G., Case, R., and Shoelson, S. E. (1994) *Biochemistry 33*, 6490−6494.
14. Stancovic, C. J., Surendran, N., Lunney, E. A., Plummer, M. S., Para, K. S., Shahripour, A., Fergus, J. H., Marks, J. S., Herrera, R., Hubbell, S. E., Humblet, C., Saltiel, A. R., Stewart, B. H., and Sawyer, T. K. (1997) *Bioorg. Med. Chem. Lett. 7*, 1909−1912.
15. Burke, T. R., Jr., Nomizu, M., Otaka, A., Smyth, M. S., Roller, P. P., Case, R. D., Wolf, G., and Shoelson, S. E. (1994) *Biochem. Biophys. Res. Commun. 201*, 1148−1153.
16. Eaton, S. R., Cody, W. L., Doherty, A. M., Holland, D. R., Panek, R. L., Lu, G. H., Dahring, T. K., and Rose, D. R. (1998) *J. Med. Chem. 41*, 4329−4342.
17. Ye, B., Akamatsu, M., Shoelson, S. E., Wolf, G., Giorgetti-Peraldi, S., Yan, X., Roller, P. P., and Burke, T. R., Jr. (1995) *J. Med. Chem. 38*, 4270−4275.
18. Beaulieu, P. L., Cameron, D. R., Ferland, J.-M., Gauthier, J., Ghiro, E., Gillard, J., Gorys, V., Poirier, M., Rancourt, J., Wernic, D., Llinas-Brunet, M., et al. (1999) *J. Med. Chem. 42*, 1757−1766.
19. Gao, Y., Luo, J., Yao, Z.-J., Guo, R., Zou, H., Kelley, J., Voigt, J. H., Yang, D., and Burke, T. R., Jr. (2000) *J. Med. Chem. 43*, 911−920.
20. Tong, L., Warren, T. C., Lukas, S., Schembri-King, J., Betageri, R., Proudfoot, J. R., and Jakes, S. (1998) *J. Biol. Chem. 273*, 20238−20242.
21. Gao, Y., Wu, L., Luo, J. H., Guo, R., Yang, D., Zhang, Z.-Y., and Burke, T. R., Jr. (2000) *Bioorg. Med. Chem. Lett. 10*, 923−927.
22. Neel, B. G., and Tonks, N. K. (1997) *Curr. Opin. Cell Biol. 9*, 193−204.
23. Pei, D., Neel, B. G., and Walsh, C. T. (1993) *Proc. Natl. Acad. Sci. U.S.A. 91*, 1092−1096.
24. Pei, D., Lorenz, U., Klingmuller, U., Neel, B. G., and Walsh, C. T. (1994) *Biochemistry 33*, 15483−15493.
25. Beebe, K. D., Wang, P., Arabaci, G., and Pei, D. (2000) *Biochemistry 39*, 13251−13260.
26. Fu, H., Park, J., and Pei, D. (2002) *Biochemistry 41*, 10700−10709.
27. Vuister, G. W., and Bax, A. (1992) *J. Magn. Reson. 98*, 428−435.
28. Schedletzky, O., Glaser, S. J., Sorensen, O. W., and Griesinger, C. (1994) *J. Biomol. NMR 4*, 301−306.
29. Zhang, Z.-Y., Wang, Y., Wu, L., Fauman, E. B., Stuckey, J. A., Schubert, H. L., Saper, M. A., and Dixon, J. E. (1994) *Biochemistry 33*, 15266−15270.
30. Jia, Z., Barford, D., Flint, A. J., and Tonks, N. K. (1995) *Science 268*, 1754−1758.
31. Pei, D., Wang, J., and Walsh, C. T. (1996) *Proc. Natl. Acad. Sci. U.S.A. 93*, 1141−1145.

BI034076U